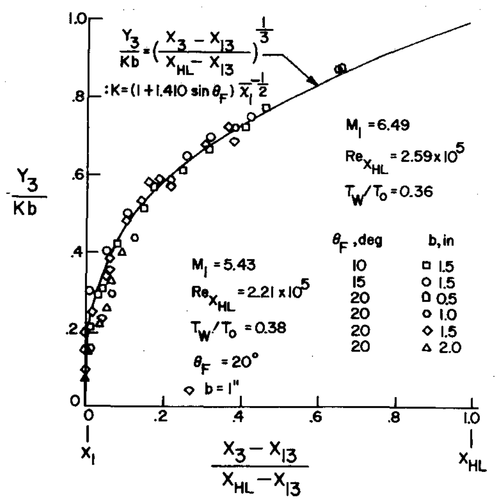

Fig. 3 Spanwise extent of separation correlation.

obtained if the boundary-layer thickness at the beginning of the interaction is used with the factor 9 changing to 10. Restating the results

$$X_{13} = X_1 = K_o M_1 \Delta\theta_F: \quad b/9\delta_{HL} \geq 1 \qquad (1)$$

where $\Delta\theta_F = \theta_F - \theta_{Fi}$ and $K_o = 0.262\, H_{tr_s}$ (Ref. 6)

$$X_{13} = (b/9\delta_{HL})X_1: \quad b/9\delta_{HL} < 1 \qquad (2)$$

Through analysis of the experimental data and recalling the shock shape prediction of the modified blast wave theory for blunt plates the following equation was obtained for the spanwise extent of separation

$$y_3/Kb = (x_3 - x_{13}/x_{HL} - x_{13})^{1/3} = X_{13}^{-1/3}(x_3/x_{13} - 1)^{1/3} \qquad (3)$$

where $K = (1 + 1.4096 \sin\theta_F)/\bar{\chi}_1^{1/2}$. It should be noted that the second term of the numerator is numerically identical to $\gamma^{1/3}C_D^{1/3}$ of the blast wave theory where $C_D = 2\sin^3\theta_F$. However, direct attainment of this functional relationship is not apparent.

Comparison of the experimental data with Eq. (3) in Fig. 3 results in excellent correlation of the experimental data over the Mach and Reynolds number range investigated.

A flap span of insufficient length, Eqs. (2) and (3), introduces departures from two-dimensionality in that the separation extent is not constant in y. These departures are related to the spanwise flow of low momentum air from the centerline, $y = 0$, in the separated region. The driving mechanism for this mass transfer is the pressure differential between the relatively high pressure in the separated region inboard of the flap, $y \leq b$, and the low pressure for $y > b$. The approximately constant separation angle for $y \leq b$ lends support to the statement that the outflow is mass transfer of low momentum air.

References

[1] Putnam, L. E., "Investigation of Effects of Ramp Span and Deflection Angle on Laminar Boundary-Layer Separation at Mach 10.03," TN D-2833, May 1965, NASA.

[2] Pate, S. R., "Investigation of Flow Separation on a Two-Dimensional Flat Plate Having a Variable-Span Trailing-Edge Flap at M = 3 and 5," AEDC TDR 64-14, March 1964, Arnold Engineering Development Center, Tullahoma, Tenn.

[3] Deitering, J. S., "Investigation of Flow Separation on a Two-Dimensional Flat Plate Having a Variable-Span Trailing Edge Flap at M = 3 and 4.5," AEDC TDR 65-59, March 1965, Arnold Engineering Development Center, Tullahoma, Tenn.

[4] Kaufman, L. G., II, Meckler, L., Hartofilis, S. A., and Weiss, D., "An Investigation of Hypersonic Flow Separation and Control Characteristics," AFFDL-TR-64-174, Jan. 1965, Air Force Flight Dynamics Lab., Wright-Patterson Air Force Base, Ohio.

[5] Ball, K. O. W., "A Summary of the Factors Influencing the Extent of Separation of a Laminar Boundary Due to a Compression Corner at Moderately Hypersonic Speeds," ARL 00-0000, April 1971, Aerospace Research Lab., Wright-Patterson Air Force Base, Ohio.

[6] Ball, K. O. W., "An Investigation of the Extent of Laminar Two-Dimensional Boundary Layer Separation at Moderately Hypersonic Speeds," Paper presented at the Symposium on Viscous Interaction Phenomena in Supersonic & Hypersonic Flow, ARL 70-1242, May 1969, Aerospace Research Lab., Wright-Patterson Air Force Base, Ohio.

Vibration Characteristics of Flexible Beams about Nonlinear Equilibrium States

George E. Weeks* and John E. Jackson†

The University of Alabama, Tuscaloosa, Ala.

Introduction

EXTREMELY flexible cantilever beam configurations have found numerous applications recently as energy dissipating devices, communications antenna, and deployable booms for space applications. In a typical loading environment such flexible members can experience large displacements away from the initially straight state. As a result of this change in geometry and the corresponding internally developed stress distribution it is expected that significant changes in the vibration characteristics of the beam will occur.

It is the purpose of this Note to present the results of an investigation on the vibration characteristics of a cantilever beam in a deformed equilibrium state after it has undergone large displacements. In order that this be accomplished the equations for infinitesimal vibrations about the equilibrium state are derived by perturbation methods, from the nonlinear equilibrium equations, and solved by numerical integration. The prestress terms, which appear as variable coefficients in these vibration equations, are obtained from the solution to the nonlinear equilibrium equations.

Problem Formulation

It is first required to derive a set of equations to describe the equilibrium state at any point along the beam. By considering a small segment of the beam as shown in Fig. 1, the following set of six nonlinear differential equations are obtained after utilizing the Kirchhoff hypothesis and assuming inextensional deformations.

$$d\bar{M}/ds = \bar{Q},\ d\bar{\theta}/ds = \bar{M}/EI \qquad (1a,b)$$

$$d\bar{T}/ds = -\bar{Q}\bar{M}/EI - p\sin\bar{\theta} + m(\ddot{\bar{w}}\sin\bar{\theta} + \ddot{\bar{u}}\cos\bar{\theta}) \qquad (1c)$$

$$d\bar{Q}/ds = \bar{T}\bar{M}/EI + p\cos\bar{\theta} - m(\ddot{\bar{w}}\cos\bar{\theta} - \ddot{\bar{u}}\sin\bar{\theta}) \qquad (1d)$$

$$d\bar{u}/ds = \cos\bar{\theta} - 1,\ d\bar{w}/ds = \sin\bar{\theta} \qquad (1e,f)$$

Here p is a "dead" distributed lateral loading, m is the mass per unit length, and dots over the symbols represent differ-

Received April 20, 1971; revision received June 2, 1971. This paper presents results of one phase of research carried out at The University of Alabama, Tuscaloosa, under U.S. Air Force Office of Scientific Research Contract F44620-69-C-0124.

Index categories: Structural Dynamic Analysis; Structural Static Analysis.

* Assistant Professor, Aerospace Engineering, Department of Mechanical Systems Engineering. Member AIAA.

† Research Assistant, Department of Mechanical Systems Engineering.

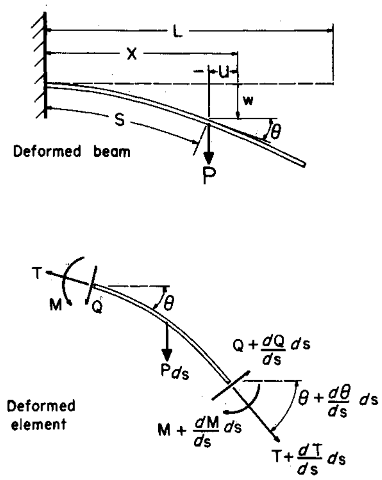

Fig. 1 Geometry of a flexible beam.

entiation with respect to time. Equations (1a–f) are valid for arbitrarily large displacements.

In order to derive the equations for the infinitesimal vibrations about the nonlinear equilibrium state, the following perturbation procedure[1] is used. Let the total moment, tension, shear, rotation, and displacements be made up of a part denoting the static equilibrium state and a part denoting the infinitesimal time dependent perturbations about this equilibrium state, then

$$\bar{M} = M_0 + M, \bar{\theta} = \theta_0 + \theta, \bar{T} = T_0 + T \quad \text{(2a,b,c)}$$

$$\bar{u} = u_0 + u, \bar{Q} = Q_0 + Q, \bar{w} = w_0 + w \quad \text{(2d,e,f)}$$

Where subscript 0 refers to the equilibrium state and the bar represents the total value of the variable. By substituting Eqs. (2a–f) into Eqs. (1a–f), subtracting out the static equilibrium state, and keeping only linear terms in the perturbed variables, there results for harmonic motion

$$dM/ds = Q, d\theta/ds = M/EI \quad \text{(3a,b)}$$

$$dT/ds = -QM_0/EI - MQ_0/EI - p\theta \cos\theta_0 - m\Omega^2(w \sin\theta_0 + u \cos\theta_0) \quad \text{(3c)}$$

$$dQ/ds = TM_0/EI + (M/EI)T_0 - p\theta \sin\theta_0 + m\Omega^2(w \cos\theta_0 - u \sin\theta_0) \quad \text{(3d)}$$

$$du/ds = -\theta \sin\theta_0, dw/ds = \theta \cos\theta_0 \quad \text{(3e,f)}$$

where Ω is the circular frequency.

Equations (3a–f) are six linear differential equations which describe the infinitesimal vibration characteristics about the nonlinear equilibrium (prestressed) state. The variable coefficients M_0, Q_0, T_0, θ_0, in these equations are functions of the prestress state and must be defined before the equations are solved. Note, importantly, that these equations contain terms involving the external loading p. For the linear case or for small deformations these terms would not be present. Note also that Eqs. (3a–f) are valid for an unstressed beam of arbitrary curvature M_0/EI and slope θ_0 if the terms T_0 and Q_0 are set equal to zero.

Table 1 Maximum values of displacements and slope for beam configurations

Diameter, in.	0.032		0.064	
Weight, lb/in.	0.2267×10^{-3}		0.9065×10^{-3}	
	linear	non-linear	linear	non-linear
Tip. defl., in. (vertical)	24.39	18.41	6.10	5.98
Tip. defl., in. (horizontal)	0	6.34	0	0.61
Slope, rad	0.96	0.77	0.24	0.24

Table 2 Natural frequency of beam configurations in radians

Diameter, in.	Mode	0.032	0.064
Classical	1	4.93	9.88
	2	31.43	62.86
	3	86.57	173.15
With prestress $p \neq 0$	1	5.58	9.97
	2	30.41	61.94
	3	84.88	173.25
With prestress $p = 0$	1	3.80	9.72
	2	30.03	61.56
	3	85.19	173.25
Curvature only $p \neq 0$	1	6.28	10.16
	2	31.28	61.94
	3	84.56	173.25
Curvature only $p = 0$	1	4.67	9.91
	2	31.09	61.94
	3	84.56	173.25

For a given beam configuration Eqs. (1a–f) were solved (neglecting the inertia terms) for the prestress quantities at equally spaced intervals along the beam using a fixed step, fourth order, Runge-Kutta integration procedure. (The application of the Runge-Kutta procedure to nonlinear boundary value problems of this type is described in detail in Ref. 2.) With the prestress variables thus defined, Eqs. (3a–f) were solved for the natural frequencies and mode shapes by numerical integration using a procedure similar to that outlined in Ref. 3.

Numerical Results

Numerical results obtained using the previously derived equations are listed in Tables 1 and 2 for two different cantilever beams of circular cross section and thirty four inches in length. The degree of nonlinearity of the equilibrium states of these beams is illustrated in Table 1 by the values of slope and vertical and horizontal displacement of the free end as calculated by linear theory and by solution of the nonlinear Eqs. (1a–f). These results were obtained by assuming the beams to be loaded by a uniformly distributed load equal to their weight per unit length. For all calculations Youngs' modulus was taken to be $E = 30 \times 10^6$ psi and 34 equally spaced intervals along the beam were used for integration. The numerical values for the displacements obtained from the nonlinear solution were validated by comparing with results obtained from experiment. In all cases, the differences were less than 2%.

In Table 2 natural frequencies are presented for the first three modes of each of the two beams as predicted by classical theory. These results were obtained from Ref. 3 and also from Eqs. (3a–f) by neglecting the weight component p and the terms associated with the prestressed state. This served as a check on the accuracy of the numerical procedure used.

The effects of the prestress state and the weight component on the frequency results are illustrated by solving Eqs. (3a–f) where both the prestress terms and the weight are included and then by solving these equations where the weight is neglected. From the results presented in Table 2, it is apparent that the effects of both prestress and weight can result in significant changes in the frequency values, for the lower modes, as the beams become more flexible.

The effects of curvature and slope on the frequency are demonstrated by solving Eqs. (3a–f) with $T_0 = Q_0 = 0$; the curvature being given by M_0/EI. The results are presented in Table 2 where it is noted that the weight component has a significant effect for the lower modes of the more flexible beam. This difference in frequency values due to the weight is attributable to the tension in the beam as a result of its deformed shape. For all frequency values presented in Table 2, the corresponding mode shapes, measured relative to the deformed equilibrium state, were almost identical to the mode shapes obtained for the classical frequencies measured relative to the undeformed (straight state).

Conclusions

The results of this investigation indicate that significant changes in the vibration characteristics of beams can occur depending on their flexibility and prestressed state. The results also showed that frequency predictions of beams by classical theory can be in considerable error if the deformed equilibrium state is such that it can only be accurately described by nonlinear theory.

Finally, the effect of the weight component on the frequencies has been shown to be significant for the more flexible beams, indicating that appropriate consideration should be given to the design of such structural components if they are to be used in a weightless environment.

References

[1] Stein, M., "The Influence of Prebuckling Stresses and Deformations on the Buckling of Perfect Cylinders," TR R-190, Feb. 1964, NASA.

[2] Weeks, G. E., "Dynamic Analysis of Stability and Deployment of Inflatable Shell Structures," Final Report BER 110-50, Jan. 1970, Univ. of Alabama, Tuscaloosa, Ala.

[3] Thomson, W. T., *Vibration Theory and Application*, Prentice-Hall, Englewood Cliffs, N.J., 1965, pp. 280–281.

Transition and Turbulence Phenomena in Supersonic Wakes of Wedges

WILHELM BEHRENS,* JOHN E. LEWIS†

AND

WILMOT H. WEBB‡

TRW Systems, Redondo Beach, Calif.

1. Introduction and Objectives

AT supersonic speeds the wake of a blunt body may be divided into an inner viscous wake stemming from the body boundary layers and an outer "inviscid" wake produced by the bow shock. In such wakes, as in the wake of a cylinder,[1] at low Reynolds numbers the onset of transition occurs thousands of diameters downstream of the body in the outer, shock-induced wake. As the Reynolds number is increased, transition occurs in the inner wake. For the same Mach number and at high Reynolds numbers transition in the wake of a wedge[2] occurs further downstream than in the case of a cylinder, but the slender body transition curve crosses the blunt body transition curve.[3] The question arises, where does transition occur in slender body wakes as the Reynolds number is decreased further? What effect does the much weaker outer shock-induced wake have on transition and, is the outer wake unstable enough to become turbulent?

Presented as Paper 70-794 at the AIAA 3rd Fluid and Plasma Dynamics Conference, Los Angeles, Calif., June 29–July 1, 1970; submitted July 24, 1970; revision received March 3, 1971. supported by the Advanced Ballistic Missile Defense Agency under Contract DAAH01-68-C-2086 and the Independent Research and Development program of TRW Systems.

Index categories: Supersonic and Hypersonic Flow; Jets, Wakes, and Viscous-Inviscid Flow Interactions.

* Consultant; also Assistant Professor of Aeronautics, California Institute of Technology, Pasadena, Calif. Member AIAA.

† Manager, Engineering Technology Department, Fluid Mechanics Laboratory.

‡ Assistant Manager, Fluid Mechanics Laboratory.

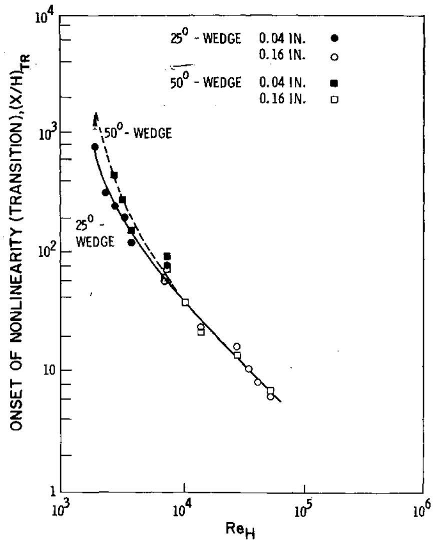

Fig. 1 Transition in wedge wakes at $M = 4.5$.

The first objective of the present work is to locate transition over a large range of Reynolds numbers in the wake of wedges and to investigate the effect of the outer, shock-induced wake on transition. Incompressible and hypersonic transitional wake flows may be divided into the linear instability region, the nonlinear instability region where a strong interaction between mean and fluctuating flow occurs, but a regular structure is still present, and the turbulent wake.[1,4,5] A study of the axial development of frequency spectra of fluctuations in these three regions is the second objective of this study.

The experiments were performed in the Jet Propulsion Laboratory's 20-in. supersonic wind tunnel at $M_\infty = 4.5$. Two wedges of 12.5° and 25° half angles, each of two sizes ($H = 0.04$ in. and 0.16 in.), were chosen for the study. The Reynolds number could be varied from $Re_H = 1900$ to 55,000. Hot wire measurements were made with a 0.0001-in. platinum-10% rhodium hot wire at constant current (for details see Ref. 3).

2. Transition Location

In the linear instability region fluctuations grow exponentially, and the mean flow still obeys the steady laminar boundary-layer equations. The wake centerline fluctuation signal is zero. Beyond a certain axial location the wake grows rapidly, indicating the onset of a strong interaction between the mean and fluctuating flow. This behavior is accompanied by the growth of fluctuations on the wake axis. This onset of nonlinearity will be called "transition." Transition location as a function of Reynolds number and wedge

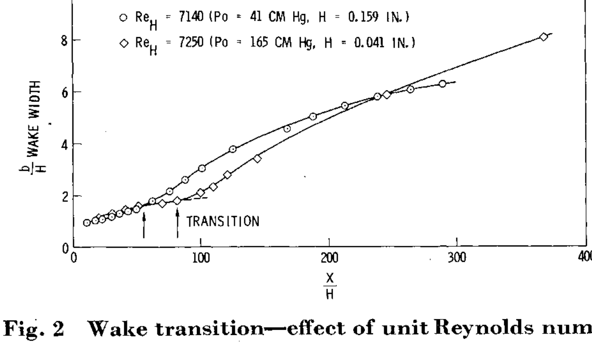

Fig. 2 Wake transition—effect of unit Reynolds number.